

NUMERICAL SIMULATION OF A DISTANT SMALL-SCALE TSUNAMI

Sung B. Yoon and Philip L.F. Liu
Cornell University
Ithaca, New York, U.S.A

ABSTRACT

An efficient numerical model is developed to simulate the propagation of distant small-scale tsunami. The model solves the linear shallow water equations using the finite element leap-frog scheme whose numerical dispersion replaces the physical dispersion of Boussinesq equations. The finite element technique has an advantage over the finite difference scheme in adjusting mesh size according to local water depth and in giving correct dispersion effects. Simulation of the 1983 Japan Sea tsunami reveals many new phenomena such as the role of the Yamato Rise and the submerged ridge as a wave guide.

INTRODUCTION

The seafloor in the Japan Sea contains active earthquake zones which have generated tsunamis causing significant damage along the Japanese coastline. These tsunamis also propagated across the Japan Sea and attacked the southeastern part of the Korean coastline.

An effective way for tsunami hazard mitigation planning is to establish inundation zones along those coastlines vulnerable to tsunami attacks. To produce reliable inundation estimates, it is essential to develop a numerical model which accurately calculates tsunami propagation from a source region to coastal areas (target regions) and the resulting tsunami run-up and flooding.

Because the earthquake zones are located along the east rim of the Japan Sea, tsunamis travel a long distance across the entire Japan Sea before reaching the east coast of Korea. The source dimension, however, is much shorter than the propagation distance. Therefore, the dispersion effects of waves are important for accurate simulation of transoceanic wave propagation.

In this study we develop a finite element model based on the leap-frog scheme to simulate tsunami propagation over a long distance. The finite element model solves the shallow water equations, but the solution given by the model contains the numerical dispersion which plays an equivalent role of physical dispersion of the Boussinesq equations. The numerical model is verified using known analytical solutions and tide gauge records for the 1983 Japan Sea Central Region Earthquake Tsunami.

GOVERNING EQUATION

If the wave length of a tsunami is long in comparison with typical water depth but is much shorter than the tsunami propagation distance, the dispersion effects are important. Since the nonlinearity is negligibly small except for the regions very near the shore, the linear Boussinesq equations can be used for the most part of the open sea. A

conservative form of Boussinesq equations for the case of slowly varying topography can be written as:

$$\eta_t + p_x + q_y = 0 \quad (1)$$

$$p_t + gh\eta_x = -\frac{gh^3}{3}(\eta_{xx} + \eta_{yy})_x \quad (2)$$

$$q_t + gh\eta_y = -\frac{gh^3}{3}(\eta_{xx} + \eta_{yy})_y \quad (3)$$

where p and q are the flux components in the x and y directions, respectively, h denotes water depth and η represents free surface displacement. The subscripts represent partial differentiation. For the unidirectional (1-D) tsunami waves over constant depth, the linear Boussinesq equations can be reduced as:

$$\eta_t + p_x = 0 \quad (4)$$

$$p_t + gh\eta_x = -\frac{gh^3}{3}\eta_{xxx} \quad (5)$$

which gives the following dispersion relationship for a periodic wave train:

$$C \equiv \frac{\omega}{k} = \sqrt{gh} \sqrt{1 - \frac{k^2 h^2}{3}} \quad (6)$$

where C is the phase speed and ω and k are the frequency and wave number, respectively. The inclusion of dispersion in Boussinesq equations gives a slower phase speed for $k \neq 0$ than that of infinitely long waves (i.e., $k = 0$).

NUMERICAL SCHEME

The leap-frog scheme has been widely employed to simulate short wave propagation over long distances due to its nondissipative nature. However, the leap-frog scheme is subject to numerical dispersion whose effect on propagating short waves is similar to that of physical dispersion. In this study we employ the leap-frog scheme to solve shallow water equations rather than Boussinesq equations and the physical dispersion effect will be represented by numerical dispersion by adjusting the step size according to the time step and local water depth as:

$$\Delta x = \sqrt{4h^2 + gh\Delta t^2} \quad (7)$$

This scheme was first introduced by Imamura (1989) in the framework of a finite difference leap-frog scheme with a staggered mesh.

It is, however, difficult to generate finite difference meshes which satisfy the condition (Eq. (7)) for the cases of a variable depth in two dimensions. To overcome this

shortcoming associated with the finite difference scheme, a finite element scheme is developed to solve the linear shallow water equations:

$$\eta_t + p_x + q_y = 0 \quad (8)$$

$$p_t + gh\eta_x = 0 \quad (9)$$

$$q_t + gh\eta_y = 0 \quad (10)$$

In this study, the Galerkin finite element method is employed to solve the shallow water equation (8)-(10). The flow field is divided into linear triangular elements. The free surface displacement, η , and flux components, p and q , are interpolated as:

$$\eta = \Phi_\alpha \eta_\alpha, \quad p = \Phi_\alpha p_\alpha, \quad q = \Phi_\alpha q_\alpha \quad (11)$$

where Φ denotes the linear interpolation function and the variables with subscript α ($= 1, 2, 3$) represent the value at the α th node of each element. The Galerkin procedure gives the following finite element equations:

$$M_{\alpha\beta} \dot{\eta}_\beta + B_{\alpha\beta} P_\beta + C_{\alpha\beta} Q_\beta = 0 \quad (12)$$

$$M_{\alpha\beta} \dot{P}_\beta + R_{\alpha\beta\gamma} h_\beta \eta_\gamma = 0 \quad (13)$$

$$M_{\alpha\beta} \dot{Q}_\beta + S_{\alpha\beta\gamma} h_\beta \eta_\gamma = 0 \quad (14)$$

where the dot denotes the time derivative and

$$\begin{aligned} M_{\alpha\beta} &= \int_{\Omega} (\Phi_\alpha \Phi_\beta) d\Omega \\ B_{\alpha\beta} &= \int_{\Omega} (\Phi_\alpha \Phi_{\beta,x}) d\Omega \\ C_{\alpha\beta} &= \int_{\Omega} (\Phi_\alpha \Phi_{\beta,y}) d\Omega \\ R_{\alpha\beta\gamma} &= g \int_{\Omega} (\Phi_\alpha \Phi_\beta \Phi_{\gamma,x}) d\Omega \\ S_{\alpha\beta\gamma} &= g \int_{\Omega} (\Phi_\alpha \Phi_\beta \Phi_{\gamma,y}) d\Omega \end{aligned} \quad (15)$$

The time derivatives are approximated by the central difference scheme, for example,

$$\eta_\beta = \frac{\eta_\beta^{n+1} - \eta_\beta^{n-1}}{2\Delta t} \quad (16)$$

where the superscript n denotes time step and all the spatial derivatives are evaluated at the n th time step. Substituting time derivatives into Eqs. (12)-(14) gives:

$$M_{\alpha\beta}^* p_{\beta}^{n+1} = M_{\alpha\beta}^* p_{\beta}^{n-1} - 2\Delta t R_{\alpha\beta\gamma} h_{\beta} \eta_{\gamma}^n \quad (18)$$

$$M_{\alpha\beta}^* q_{\beta}^{n+1} = M_{\alpha\beta}^* q_{\beta}^{n-1} - 2\Delta t S_{\alpha\beta\gamma} h_{\beta} \eta_{\gamma}^n \quad (19)$$

where $M_{\alpha\beta}^*$ is the lumped coefficient matrix obtained by row sum of $M_{\alpha\beta}$ to ensure the pure explicit scheme.

The 1-D version of finite element equations (17)-(19) for a constant depth can be represented in the following form:

$$\frac{\eta_i^{n+1} - \eta_i^{n-1}}{2\Delta t} + \frac{p_{i+2}^n - p_{i-1}^n}{2\Delta x} = 0 \quad (20)$$

$$\frac{p_i^{n+1} - p_i^{n-1}}{2\Delta t} + \frac{\eta_{i+2}^n - \eta_{i-1}^n}{2\Delta x} = 0 \quad (21)$$

where the subscript i represents spatial step and the superscript n denotes time step. Using the Taylor series expansion, Eqs. (20) and (21) can be recast into differential equations:

$$\eta_i + p_x = 0 \quad (22)$$

$$p_t + gh\eta_x = -\frac{gh\Delta x^2}{3}(1-v^2)\eta_{xxx} + O(\Delta t^4, \Delta x^4, \Delta t^2, \Delta x^2) \quad (23)$$

where v is the Courant number defined by:

$$v = \sqrt{gh} \frac{\Delta t}{\Delta x} \quad (24)$$

The right-hand side of Eq. (23) represents the numerical dispersion error resulting from the finite element approximation of shallow water equations through the leap-frog scheme. These modified equations give the dispersion relationship for a periodic wave as:

$$C = \frac{\omega}{k} = \sqrt{gh} \sqrt{1 - \frac{k^2 \Delta x^2}{3}(1-v^2)} \quad (25)$$

The above dispersion relationship becomes the same as that given by Boussinesq equations (6) if we define

$$\Lambda x = \sqrt{h^2 + gh\Delta t^2} \quad (26)$$

which is slightly different from the condition (7) given by Imamura (1989) due to the different definition of step sizes. For the two-dimensional cases this condition gives slightly less numerical dispersion for the waves propagating obliquely to the mesh alignment than along the main axes (see Imamura & Goto, 1988).

TEST OF NUMERICAL MODEL

To verify the accuracy of the finite element model, tsunami waves propagating radially in two dimension over a horizontal bottom ($h = 10$ m) are simulated. The initial free surface displacement η is given by Gaussian hump centered at the origin ($x = y = 0$) as:

$$\eta(x, y, t = 0) = 2e^{-(x^2+y^2)/a^2} \quad (27)$$

where a , the characteristic width of Gaussian hump, is set to be 50 m.

The exact solution of a linear KdV equation is given by Carrier (1990) as:

$$\eta(r, t) = \int_0^\infty \rho J_0(\rho r) \cos\left(\frac{\rho t}{\sqrt{1+h^2\rho^2/3}}\right) e^{-\rho^2/4} d\rho \quad (28)$$

where $r (= \sqrt{x^2 + y^2} / a)$ is the normalized distance from the origin, J_0 is the Bessel function of the first kind of order zero. The integration is performed numerically using Gaussian quadratures. As shown in Figure 1, the uniform mesh size $\Delta x (= \Delta y)$ is chosen as 14.142 m which satisfies the condition (26) according to the time step $\Delta t = 1$ sec. and water depth $h = 0$ m.

Figure 2 shows the comparison between exact and numerical solution at 300 sec. Numerical solutions are presented along the x -axis (OA), the y -axis (OC) and the diagonal line (OB) (see Figure 1). The numerical result shows stronger dispersion effects than the exact solution in all directions of propagation, and this dispersion effect seems to decrease when the waves propagate obliquely to the main axes as predicted by Imamura & Goto (1988). The finite element leap-frog scheme gives reasonable solutions for leading waves, but slight deviations for the tail of wave group.

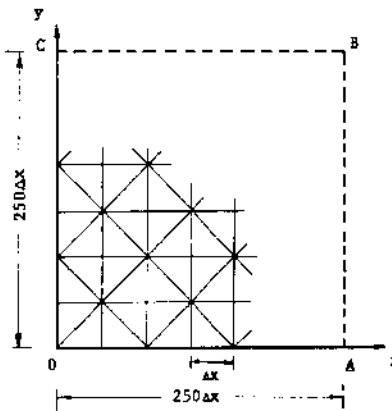


Figure 1. Finite element mesh for model test

SIMULATION OF 1983 JAPAN SEA TSUNAMI

For verification of numerical models developed in this study, the 1983 Japan Sea Central Region Earthquake Tsunami (1983 Tsunami hereafter) is simulated. The Japan Sea is bordered by Russia and Korea on the northwest and by Japan on the southeast as shown in Figure 3. Its dimension is roughly 1200 km x 1200 km. Since the source area of the tsunami is small (30 km x 100 km) in comparison with the entire Japan Sea and the bathymetry is complicated due to the presence of submerged rises and ridges, the finite element model has an advantage over the finite difference model in satisfying Eq. (26) everywhere for the correct dispersion effect.

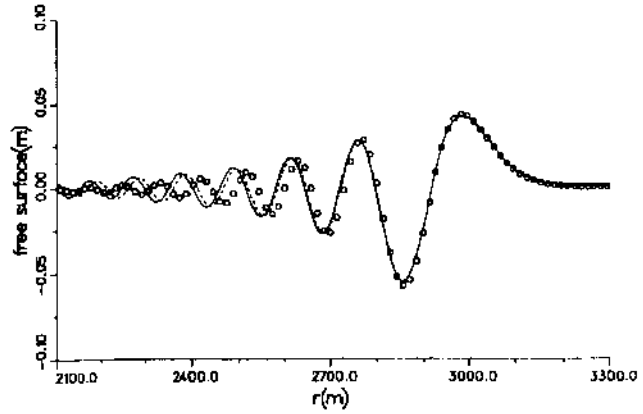


Figure 2. Comparison of free surface displacements at 300 sec.
 oooo analytical
 --- numerical along x & y axes
 numerical along y=x

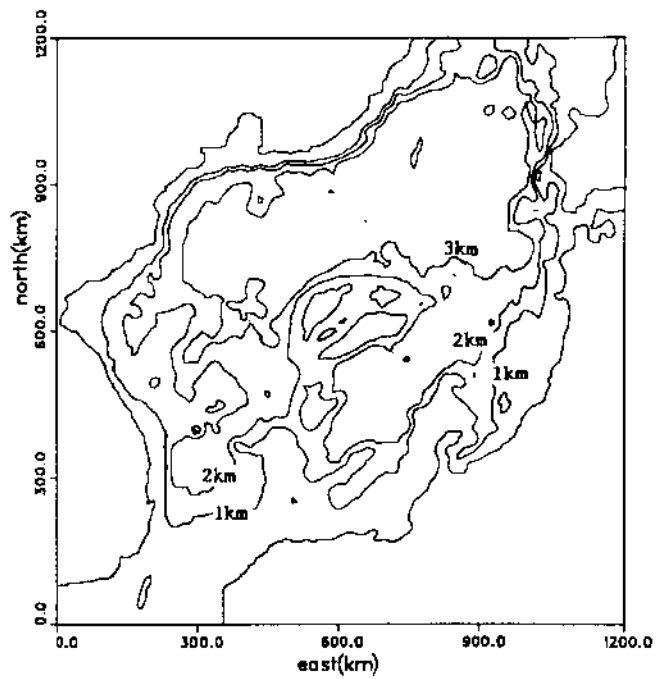


Figure 3. Bathymetry of the Japan Sea

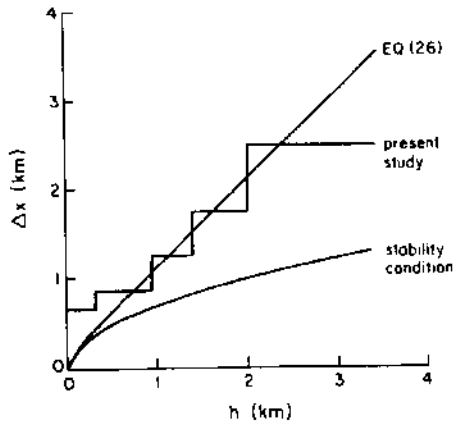


Figure 4. Finite element mesh size based on time step 5 sec.

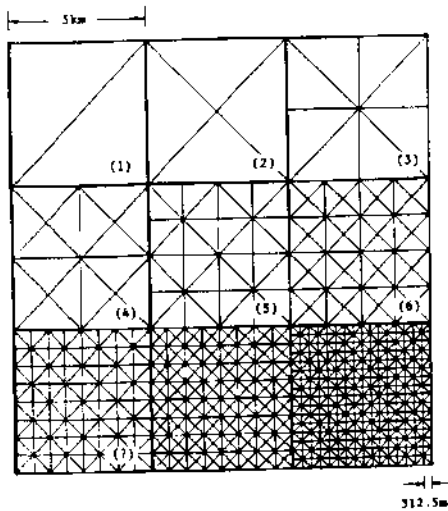


Figure 5. Finite element mesh employed in simulation of 1983 Tsunami

Figure 4 shows the mesh size determined by Eq. (26) for different water depths associated with the given time step of 5 sec. The entire Japan Sea is discretized into 629,147 triangular elements with 317,372 nodes using the first seven types of elements as shown in Figure 5. The distribution of these elements is shown in Figure 6.

To obtain the initial displacement of water surface due to the 1983 Tsunami, the fault parameters of Aida model-10 are employed (Aida, 1984). The vertical displacement of sea bottom at the source area is calculated using the theory of Mansinha and Smylie (1971) and is assumed to be the same as that of the water surface. All the flux components, p and q , are assumed as zero.

The arrival times of the leading wave from simulation are compared with tide gauge record along the southeast coast of Korea and along the northwest coast of Japan in Figures 7 and 8 where the locations are shown in Figure 9. Except for a few locations, the agreement between observed and calculated arrival times are good.

Figure 10 shows the distribution of highest water level obtained from the numerical simulation. The northern Akita coast of Japan (JA) is expected to have the largest wave heights due to the orientation of source and short distance from the source. The main waves propagating over the Yamato Rise (YM) are converged behind the rise and trapped along the submerged ridge joining Yamato Rise and Shimane Peninsula (JF) of Japan. Some portions of the main waves travel toward the east coast of Korea (KA). As a result three main peaks develop near North Akita Coast (JA), Shimane Peninsula (JF), and the east coast of Korea (KA). More local peaks appear at the Yamagata region (JB), the north part of Sado Island (JC), Noto Peninsula (JD), and the Tsuyama-Maizuru region (JE).

The mesh size used near shore is too coarse to give quantitative agreement with tide gauge records, since the tide gauges are usually located deep inside a harbour

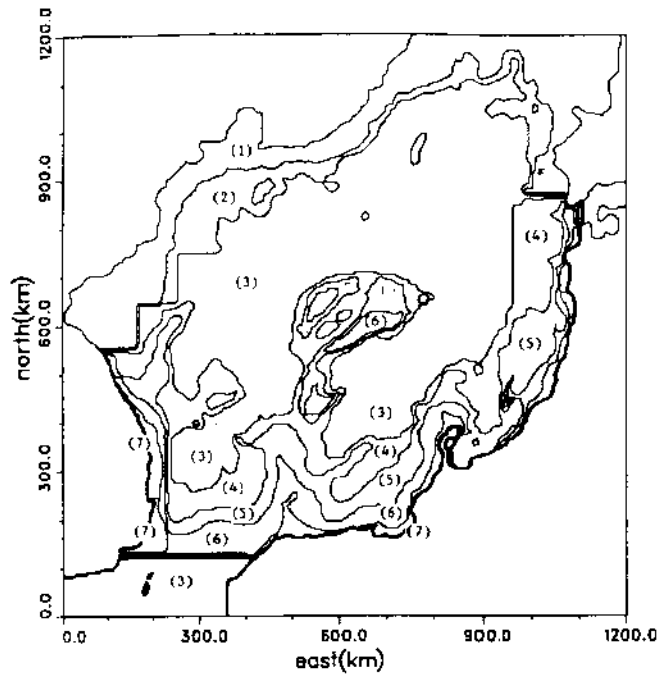


Figure 6. Finite element discretization of Japan Sea for the simulation of the 1983 Tsunami

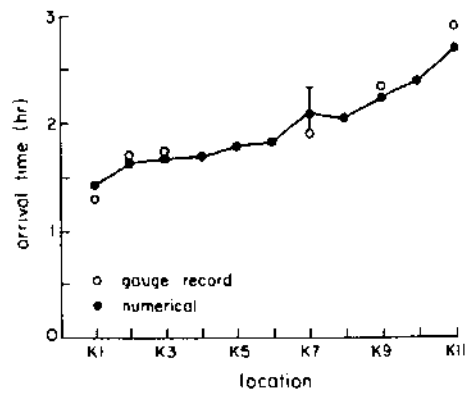


Figure 7. Comparison of arrival time along east coast of Korea (see Figure 9 for locations)

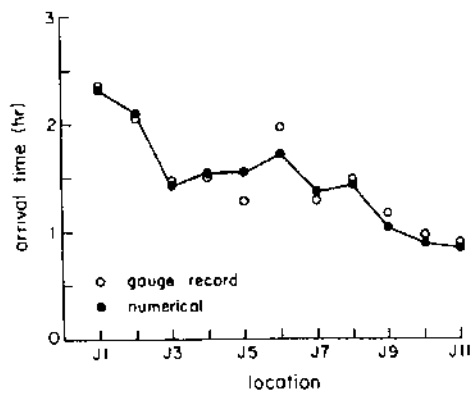


Figure 8. Comparison of arrival time along east coast of Japan (see Figure 9 for locations)

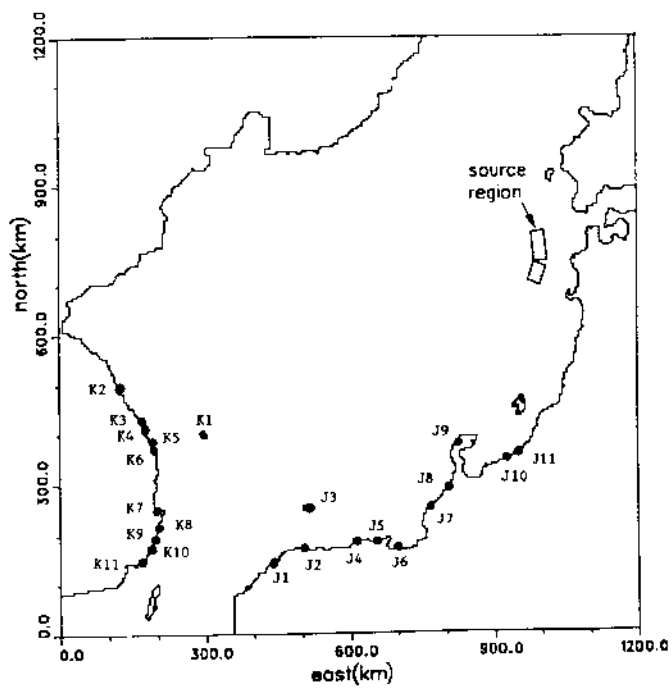


Figure 9. Location of arrival time checking stations

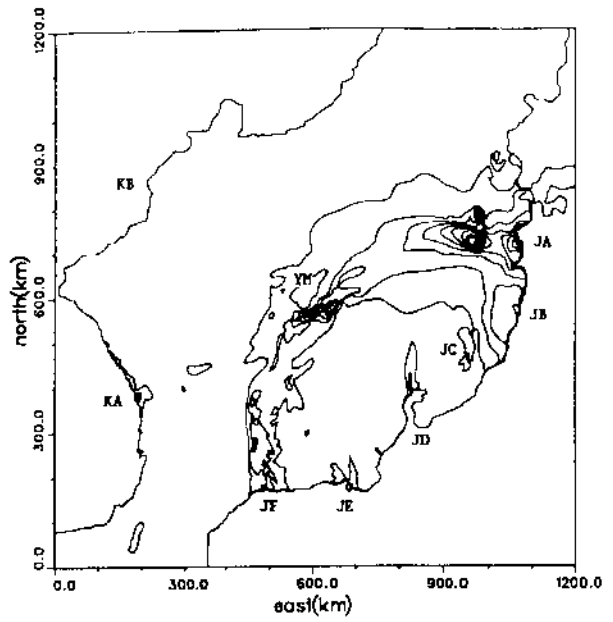


Figure 10. Distribution of computed highest water levels with contour increment of 0.25 m

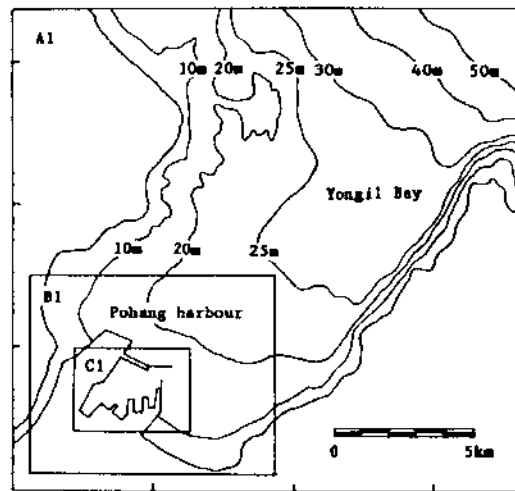


Figure 11. Bathymetry near Pohang Harbour of Korea

protected by coastal structures. For the detailed local computations, the finite difference model developed by Shuto, et al. (1986) is employed. The finite difference model solves the full shallow water equations based on the leap-frog scheme with staggered mesh. Some special features such as wave run-up, overtopping, and nesting etc., are also included in the model to study the interaction of tsunamis with complicated geometry.

The Pohang Harbour located at the southeast coast of Korea is chosen to verify the detailed finite difference model. The bathymetry near Pohang Harbour is presented in Figure 11 which shows three regions, A1, B1 and C1, for the nesting of different mesh size regions. The mesh sizes are 625 m, 208.33 m, and 69.44 m for A1, B1, and C1 regions, respectively. The time step is 1 sec. The time history of fluxes and free surface displacement obtained from the finite element model is prescribed along the open boundaries of the computational domain (A1 region).

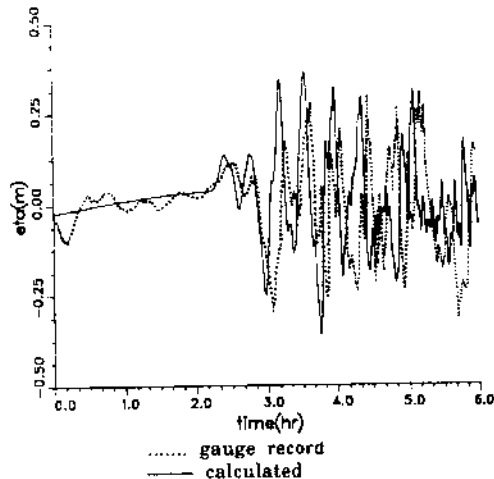


Figure 12. Comparison of water surface elevation time history at gauge station of Pohang Harbour

The calculated time history of water surface at the tide gauge station inside the harbour is compared with the gauge record in Figure 12 for 6 hours after generation of the 1983 Tsunami. The tide gauge record shows some wind waves (wave height of 12.5 cm) and tides before the tsunami wave arrives at the harbour. The first two waves are smaller than the third wave due to the dispersion effect of waves described earlier. This shows clearly that the dispersion effect is important for accurate prediction of a distant tsunami. The predominant period of tsunami waves is approximately 25 min. for both cases of numerical and recorded time histories, while the tide gauge records of other locations along east coast of Korea show much shorter wave periods (10-15 min.)

The calculated highest water level gives larger values than the recorded one by 5 cm and the lowest water level from computation is 4 cm lower than observed one. The calculated wave arrives at the gauge point earlier by 5 cm and continuously leads the phase of recorded wave. This discrepancy of wave height and phase could be explained by the characteristics of tide gauge itself (Lander & Lockridge, 1990). The agreement between numerical prediction and tide gauge record is reasonable if the pre-existing wind wave and the tide gauge characteristics are taken into consideration.

CONCLUDING REMARKS

The finite element model developed in this study is shown to be efficient and accurate to simulate the propagation of distant small-scale tsunamis where the dispersion effect is important. The model can be used in conjunction with other detailed run-up models to establish inundation maps for the areas vulnerable to tsunami attacks

The numerical simulation of the 1983 Tsunami shows that the Yamato Rise acts as a focusing lens and the submerged ridge connecting Yamato Rise to Shimane Peninsula of Japan plays the role of a wave guide. These topographic changes should be taken into account for the accurate estimation of tsunami wave heights for the areas of the east coast of Korea and the west part of Japan.

ACKNOWLEDGMENT

This research was carried out with support from the Korea Power Engineering Company and the National Science Foundation. The finite difference detail model was kindly provided by Dr. N. Shuto and Dr. F. Imamura of Tohoku University, Japan. The 3-D animation of the 1983 Tsunami was made by Miss Catherine Devine of Cornell Theory Center.

REFERENCES

- Aida, I. 1984. A source model of the tsunami accompanying the 1983 Nihonkai-Chubu earthquake. *Bull. Earthq. Res. Inst.* **59**:235-265. (in Japanese)
- Carrier, G.F. 1991. Tsunami propagation from a finite source. In: Proc. of 2nd UJNR Tsunami Workshop, NGDC, Honolulu, Hawaii. pp. 101-115.
- Imamura, F. 1989. Possibility of tsunami numerical forecasting. Ph.D. diss., Tohoku University (in Japanese).
- Imamura, F., and C. Goto. 1988. Truncation error in numerical tsunami simulation by the finite difference method. *Coastal Engineering in Japan*. **31(2)**:245-263.
- Lander, J.F., and P.A. Lockridge. 1990. United States Tsunamis (including United States Possessions) 1690-1988. National Geophysical Data Center, Boulder, Colorado.
- Manshinha, L., and D.E. Smylie. 1971. The displacement fields of inclined faults. *Bull. Seism. Soc. Am.* **61**:1433-1440.
- Shuto, N., T. Suzuki, K. Hasegawa, and K. Inagaki. 1986. A study of numerical technique on the tsunami propagation and run-up. *Science of Tsunami Hazards, the Intl. J. of the Tsunami Society*. **4(2)**:111-124.